Characterizations and comparison of low sulfur fuel oils compliant with 2020 global sulfur cap regulation for international shipping

Robert K. Nelson [a], Alan G. Scarlett [b,*], Marthe Monique Gagnon [c], Alex I. Holman [b], Christopher M. Reddy [a], Paul A. Sutton [d], Kliti Grice [b,*]

[a] Department of Marine Chemistry and Geochemistry, Woods Hole Oceanographic Institution, Massachusetts, MA 02543, USA
[b] Western Australian Isotope and Geochemistry Centre, School of Earth and Planetary Sciences, Curtin University, Perth 6102, Australia
[c] School of Molecular and Life Sciences, Curtin University, Perth 6102, Australia
[d] Biogeochemistry Research Centre, School of Geography Earth & Environmental Sciences, University of Plymouth, Plymouth, England, United Kingdom of Great Britain and Northern Ireland

ARTICLE INFO

ABSTRACT

The International Marine Organization 2020 Global Sulfur Cap requires ships to burn fuels with <0.50% S and some countries require <0.10% S in certain Sulfur Emission Control Areas but little is known about these new types of fuels. Using both traditional GC–MS and more advanced chromatographic and mass spectrometry techniques, plus stable isotopic, $\delta^{13}C$ and δ^2H, analyses of pristane, phytane and n-alkanes, the organic components of a suite of three 0.50% S and three 0.10% S compliant fuels were characterized. Two oils were found to be near identical but all of the remaining oils could be forensically distinguished by comparison of their molecular biomarkers and by the profiles of the heterocyclic parent and alkylated homologues. Oils could also be differentiated by their $\delta^{13}C$ and δ^2H of n-alkanes and isoprenoids. This study provides important forensic data that may prove invaluable in the event of future oil spills.

1. Introduction

Spillages of fuel oil from ships have occurred frequently throughout modern history and are relatively common compared with releases of crude oil (Jernelov, 2010), some of these spills have been well studied (e.g. Chen et al., 2018; Fingas, 2016; Lemkau et al., 2010; Nelson et al., 2006; Radovic et al., 2014). Compared to these previous fuel oil releases, the oil spill that resulted from the grounding of the MV *Wakashio* in July 2020 was unremarkable except that it represented the first major spillage of Very Low Sulfur Fuel Oil (VLSFO) since the introduction of a new Global Sulfur Cap regulation was implemented from January 2020 (IMO, 2020; Scarlett et al., 2021). An agency of the United Nations known as the International Marine Organization (IMO), which is responsible for regulating the marine sector world-wide, mandated a protocol which requires shippers to transition to "Low-Sulfur Fuels" in 2011 requiring implementation by the Marine Sector on January 1, 2020 (IMO, 2020). Colloquially known as IMO-2020, the IMO's new shipping regulations refer to Annex VI of the International Convention for the Prevention of Pollution from Ships (MARPOL). IMO-2020 was primarily put into effect in order to reduce air pollution in Emission Control Areas

(ECA's) caused by the burning of marine fossil fuels; more specifically, to reduce the emissions of sulfur-oxide (SO$_x$) and nitrous-oxide (NO$_x$) compounds and particulates (IMO, 2020). IMO-2020 guidelines lowered the allowable weight percentage of sulfur from 3.5 wt% down to 0.50 wt % beginning on the January 1, 2020 implementation date. The IMO refers to fuels meeting the 0.50 wt% sulfur limit as VLSFO. There are a number of avenues available to the Marine Sector designed to meet MARPOL's low-sulfur emission goals. Marine operators can (a) install Exhaust Gas Cleaning Systems also known as "exhaust scrubbers", (b) install engines capable of burning biofuels or liquefied natural gas (LNG), or (c) utilize low-sulfur marine fuels. In addition to IMO-2020 ECA's, a number of European Union countries as well as the United States and Canada have implemented more stringent Sulfur Emission Control Areas (SECA's) requiring Marine Operators to utilize marine fuels containing a maximum of 0.10 wt% sulfur (CARB, 2020). Marine fuels meeting the 0.10 wt% sulfur criteria are known as ULSFO (Ultra Low Sulfur Fuel Oil). The compliant VLSFO and ULSFO, are replacing the traditional intermediate fuel oils or heavy fuel oils e.g. IFO 180 and IFO 380, but information about their physical and chemical characteristics are only just becoming known.

A recent study by Sørheim et al. (2021) that compared the physico-chemical characteristics of the MV *Wakashio* VLSFO, with other low S fuel oils, including both VLSFO and ULSFO, reported that neither the density (0.908 g/mL), pour point (+9 °C), nor the asphaltenes (0.52 wt %) and wax (5.4 wt%) were deemed to be outliers (Table 1). The viscosity of ~33 mPa.s (at 50 °C) reported for the *Wakashio* fuel oil was higher than marine distillates (DMA diesel) but similar to that of intermediate bunker fuel oil (IFO-30) and was in the lower range of other VLSFO, although an ULSFO was even lower (Sørheim et al., 2021). It therefore appears that in terms of bulk physico-chemical characteristics, the *Wakashio* fuel oil cannot be considered extreme. However, when considering the potential impact of VLSFO and ULSFO on the environment if spilled, and to aid with forensic discrimination, the composition of the hydrocarbon and heterocyclic components, and ideally the resins and asphaltenes, of the oils also need to be assessed.

An examination of both the *Wakashio* fuel oil and a sample of oily residue recovered from the Mauritius coast (Scarlett et al., 2021) found that they both possessed untypically low quantities of polycyclic aromatic hydrocarbons (PAH) and very low concentrations of S- and N-containing heterocyclics when compared with a large set of marine heavy fuel oils reported by Uhler et al. (2016). Some other VLSFOs and ULSFOs also appear to have relatively low quantities of PAH (Sørheim et al., 2020) so this may indicate that future spillages of IMO-2020 compliant fuel oils from ships pose less of a threat to marine organisms due to exposure to toxic PAHs.

Previous studies of fuel oil spills (e.g. Chen et al., 2018; Fingas, 2016; Lemkau et al., 2010; Nelson et al., 2006; Radovic et al., 2014; Scarlett et al., 2021) have utilized biomarker profiles to help identify the geologic origin of the spilled oil, identify/constrain the spill, and distinguish the spilled oil with background. These biomarkers i.e. molecules in petroleum derived from once-living plants and animals (Peters et al., 2005), are often found in crude oils and their products and, due to their resistance to biodegradation, are useful for characterizing petroleum contamination in the environment (Wang et al., 2016). However, sometimes the biomarkers most resistant to weathering and biodegradation, such as the steranes and hopanes, are in very low abundances or not present making identification and comparison between the source and spilled oil very challenging. It was postulated by Scarlett et al. (2021) that the profiles of some heterocyclic compounds may also be useful for identifying VLSFOs. Acquiring characterisations of heterocyclic profiles in addition to traditional biomarkers present in a range of VLSFO and ULSFO could therefore prove useful prior to future spillages that will inevitably occur. Yet, the complex nature of the oil and identifying useful molecular indicators and biomarkers demands high-resolution mass spectrometry and specificity well suited to GC × GC analyses.

Comprehensive two-dimensional gas chromatography (GC × GC), either coupled to a flame ionization detector (FID) or a mass spectrometer (MS), is an extremely powerful analysis technique capable of resolving complex mixtures of hydrocarbons and their metabolic products (e.g. Frysinger et al., 2003; Gaines et al., 1999; Nelson et al., 2016; Nelson et al., 2006; Rowland et al., 2011), even when present as weathered and biodegraded environmental contaminants. A recent advance that couples the resolving power of GC × GC with high-resolution mass spectrometry (GC × GC-HRT), has further improved characterization of oil spill samples (Nelson et al., 2019; Scarlett et al., 2021). For example, despite the very low abundances in biomarkers and S- and N-heterocyclics present in the *Wakashio* fuel oil, GC × GC-HRT analyses was able to resolve, identify and provide detailed profiles of many such compounds (Scarlett et al., 2021). Although GC × GC-HRT has many advantages over traditional GC–MS, it is not yet widely used whereas the latter is now a commonly available instrumental method in most analytical laboratories worldwide so in this study both methods have been applied.

Stable isotopes have potential to be a useful tool for identifying the source of an oil spill (Asif et al., 2011; Li et al., 2009). Although Scarlett et al. (2021) reported a reasonable similarity in ratios of both δ^{13}C and δ^2H between the spilled oil and the *Wakashio* fuel oil, some differences were observed likely due to weathering effects. Comparing δ^{13}C and δ^2H ratios for a range of IMO-2020 compliant oils could provide further information on the practical usage of stable isotopes for identifying the source of an oil spill.

In this study, we explored the molecular and isotopic complexity of three VLSFOs, two ULSFOs and a heavy marine distillate compliant with <0.10% S with traditional GC–MS, GC × GC-FID and GC × GC-HRT, high temperature GC-FID, and compound specific isotope analysis (CSIA) by gas chromatography isotope-ratio mass spectrometry (GC-irMS). The main aims of this study were to assess the variation between the oils, provide information for oil spill responders to aid rapid assessment and action, and to ascertain key features that may help identify individual fuel oils.

2. Materials and methods

2.1. Oils

Five of the six fuel oils were supplied by SINTEF (Norway). These included three VLSFOs including the fuel oil from the MV *Wakashio* previously analysed by Scarlett et al. (2021), an ULSFO and a SECA compliant distillate heavy marine gas oil with <0.10% S. Labelling for these VLSFOs and ULSFO is in accordance with that used by Sørheim et al. (2021). The distillate heavy marine gas oil is labelled HMGO-1. Readers are directed to Sørheim et al. (2020, 2021) for more detailed descriptions and physico-chemical properties of the oils supplied by SINTEF; selected values are reproduced in Table 1. An additional ULSFO was sourced independently from an oil company that did not supply samples to SINTEF. Physico-chemical properties of the latter, labelled ULSFO-3, are not yet available.

Aliquots of the oils were distributed to Curtin University, Plymouth University and Woods Hole Oceanographic Institution. Methods were generally as described by Scarlett et al. (2021).

Table 1
Asphaltene, wax and selected physical properties of VLSFOs, ULSFOs, HMGO and two traditional heavy fuel oils. Reproduced from Sørheim et al. (2020, 2021).

Oil types	Asph (wt%)	Wax (wt%)	Density (g/mL)	Pour point (°C)	Visc. (mPa.s)[b] 50 °C 10s^{-1}	Visc. (mPa.s) 13 °C 10s^{-1}	Visc. (mPa.s) 13 °C 100 s^{-1}
Wakashio	0.52	5.4	0.908	9[a]	~33	1199	582[c]
VLSFO-1	0.44	4.5	0.989	9	~50	5550	3948
VLSFO-2	4.8	4.9	0.990	3	~350	19,450	16,507
ULSFO-2	0.14	20.7	0.917	24	~70	33,564	5986
HMGO-1	0.06	9.5	0.903	12	~45	1005	–
IFO 180	5.7	4.4	0.973	6	–	7426	5118
IFO 380	6.6	5.6	0.990	−6	~480	27,294	21,909

[a] Estimated data.

[b] Interpolated from Figs. 5-3 Sørheim et al. (2020) except Wakashio VLSFO as stated in Sørheim et al. (2021).

[c] Viscosities millipascal second (mPa.s) measured at 13 °C except Wakashio VLSFO conducted at 15 °C with shear rates (s^{-1}) of 10 or 100 s^{-1}. ULSFO-3 was not included in the cited studies.

2.2. GC–MS

Saturate fractions (100% *n*-hexane) of the oils were separated by silica gel chromatography. Analyses were performed using a HP-6890A gas chromatograph (Agilent, Santa Clara, CA, USA) interfaced to a HP-5973 mass selective detector (Agilent) fitted with a DB-1 ms capillary column (60 m × 0.25 mm internal diameter × 0.25 μm film thickness). The GC oven was programmed from 40 °C (held 2 min) to 320 °C at 6 °C min^{-1} with a final hold time of 26 min. Ultra-high purity helium was used as the carrier gas with a constant flow of 1 mL min^{-1}. Sample injection was 1 μL pulsed splitless at 280 °C. The MSD was operated at 70 eV with a source temperature of 230 °C. Mass spectra were acquired in full scan mode and with selected ion monitoring (SIM, *m/z* 123, 191, 205, 217, 218, 358, 370, 372, 384, 386, 398, 400, 412, 414, 426, 428, 440, 442, 454, 456). Identification of biomarkers was aided by reference to certified analytical standards (NIST SRM-2266, Gaithersburg, MD, USA).

2.3. HTGC

High temperature GC-FID was utilized to detect high-molecular-weight components not observed with normal range GC. A 0.5 μL sample aliquot was 'hot' (sample and syringe pre-heated at 70 °C) manually injected via a cool-on-column inlet (track oven mode; +3 °C) onto a Vf-5ht Ultimetal column (15 m × 0.25 mm × 0.1 μm; Agilent Technologies Limited, UK) operated with He carrier gas (constant flow mode; 1 mL min^{-1}) and the GC oven (HP6890) programmed from 40 to 430 °C at 10 °C min^{-1} with 10 min isothermal hold. The FID high temperature jet was operated at 430 °C (FID gas flows optimized at H$_2$ 40 mL min^{-1}, air 450 mL min^{-1} and N$_2$ make-up 45 mL min^{-1}).

2.4. GC×GC-FID

Analyses were performed on a LECO instrument consisting of an Agilent 7890A GC configured with a split/splitless auto-injector (7683B series) and a dual stage cryogenic modulator (LECO, Saint Joseph, Michigan). The GC × GC-FID carrier gas was hydrogen (H$_2$) at a flow rate of 1 mL min^{-1} and the instrument was operated in constant flow rate mode. Samples were injected in splitless mode. Samples were prepared at a concentration of 5 mg mL^{-1} neat fuel in CH$_2$Cl$_2$. The cold jet gas was dry N$_2$ chilled with liquid N$_2$. The hot jet temperature offset was 5 °C above the temperature of the secondary GC oven and the inlet temperature was isothermal at 310 °C. Two capillary GC columns were utilized for these GC × GC analyses. The first-dimension column was a Restek Rxi-1 ms, (60 m length × 0.25 mm × 0.25 μm) and second-dimension separations were performed on a 50% phenyl polysilphenylene-siloxane column (SGE BPX50, 1.2 m × 0.10 mm × 0.1 μm). The temperature program of the main oven was held isothermal at 65 °C (12.5 min) and was then ramped from 65 to 340 °C at 1.25 °C min^{-1}. The second-dimension oven was held isothermal at 70 °C (12.5 min) and then ramped from 70 to 345 °C at 1.25 °C min^{-1}. The hot jet pulse width was 1 s, and the modulation period between stages was 6.5 s and a cooling period of 2.25 s between stages. FID data was sampled at an acquisition rate of 100 data points s^{-1}.

2.5. GC×GC-HRT

High resolution analyses by GC × GC-HRT utilized a LECO Pegasus GC × GC-HRT 4D instrument consisting of an Agilent 7890B GC configured with a LECO LPAL3 split/splitless auto-injector and a dual stage cryogenic modulator (LECO, Saint Joseph, Michigan). The carrier gas was He at a flow rate of 1 mL min^{-1} in constant flow mode. Samples were prepared at a concentration of 5 mg mL^{-1} neat fuel in CH$_2$Cl$_2$ and were injected in splitless mode. The cold jet gas was dry N$_2$ chilled with liquid N$_2$. The hot jet temperature offset was 15 °C above the secondary oven and the inlet temperature was isothermal at 310 °C. The first-dimension column was a Restek Rxi-1 ms, (60 m × 0.25 mm × 0.25 μm) and second-dimension separations were performed on a 50% phenyl polysilphenylene-siloxane column (SGE BPX50, 1.2 m × 0.10 mm × 0.1 μm). The temperature program of the main oven was held isothermal at 80 °C (12.5 min) and was then ramped to 330 °C at 1.25 °C min^{-1}. The second-dimension oven was held isothermal at 85 °C (12.5 min) and then ramped from 85 to 345 °C at 1.25 °C min^{-1}. The hot jet pulse width was 2 s, and the modulation period between stages was 8 s with a cooling period of 2 s between stages. HRT data was sampled at an acquisition rate of 200 spectra s^{-1}. The ionization method was electron ionization (EI) with an electron energy of −70 eV and an extraction frequency of 1.5 kHz.

2.6. GC-irMS

Saturate fractions were obtained as for GC–MS but without the addition of perdeuterated standards. δ^{13}C and δ^2H of *n*-alkanes and isoprenoids pristane and phytane was performed using a Thermo Delta V Advantage irMS, coupled to a Thermo Trace GC Ultra via a GC Isolink and Conflo IV. The irMS measured fragment ions *m/z* 44, 45 and 46 for CO$_2$ or *m/z* 2 and 3 for H$_2$. The δ^{13}C and δ^2H values were calculated from the measured masses by Thermo Isodat software. Values were converted to the VPDB/VSMOW scales by comparison with an in-house mixture of *n*-alkane standards (*n*-C$_{11}$, *n*-C$_{13}$, *n*-C$_{14}$, *n*-C$_{17}$, *n*-C$_{18}$, *n*-C$_{19}$ and *n*-C$_{25}$) of known isotopic composition (δ^{13}C from −25.3 to −32.2‰, δ^2H from −104.2 to −268.6‰), and commercially available isotopic standards from Indiana University (http://pages.iu.edu/~aschimme/hc.html): *n*-C$_{22}$ (δ^{13}C -32.87 ± 0.03‰, δ^2H -62.8 ± 1.6‰) and squalane (δ^{13}C -20.49 ± 0.02‰ and δ^2H -168.9 ± 1.9‰). Samples were measured in triplicate, and standard errors were less than 0.5‰ for δ^{13}C and generally 5‰ for δ^2H.

3. Results and discussion

3.1. Characterization of saturate fractions of oils by GC–MS

Total Ion Chromatograms (TIC) produced by traditional Full Scan GC–MS analysis of the suite of IMO-2020 compliant oils clearly showed a large degree of variation in the alkane profiles of the oils with the exception of ULSFO-2 and ULSFO-3 which appeared very similar (Fig. 1). Only the *Wakashio* oil possessed the most abundant *n*-alkane peak below *n*-C$_{20}$ (Fig. 1). A large underlying unresolved complex mixture (UCM) of high weight components was apparent in the VLSFO-2 and, to a lesser extent, in HMGO-1 (Fig. 1). Following an oil spill and subsequent weathering, alkane profiles rapidly change, initially due to evaporative losses (which can also occur during sample work-up), but later biodegradation can also become significant, and the biomarker profiles are more useful for forensic 'fingerprinting' (Wang et al., 2016). Ratios of the isoprenoids pristane (Pr) and phytane (Ph), and their corresponding *n*-alkanes, are commonly applied to oil fingerprinting but the *n*-alkanes may be more greatly altered due to such weathering effects once an oil enters the environment. Comparing chromatographic areas from TIC, some oils possessed similar values for individual ratios, but the only oils that were similar for all ratios were ULSFO-2 and ULSFO-3 (Table 2). All of the ratios for *n*-C$_{17}$/Pr were in the Min-Max range of 0.6–3.0 reported for 71 IFO 380 HFOs, whereas only HMGO-1 was in the range of 1.2–2.9 for *n*-C$_{18}$/Ph (Uhler et al., 2016). In a crude oil, Pr/Ph ratios ranging between 1 and 3 are generally thought to reflect oxidizing depositional environments (Peters et al., 2007). VLSFO-2 and both ULSFOs fit into this category. The very high Pr/Ph ratio of 3.25 in the *Wakashio* VLSFO suggests a feedstock oil with a terrestrial origin and the low ratio of 0.63 for HMGO-1 (Table 2) is normally associated with a reducing depositional environment (Peters et al., 2007). However, feedstock oils may be mixtures of multiple crude oils and refinery processes are known to alter various biomarker ratios (Peters et al., 1992), so any such interpretation of biomarker ratios of fuel oils should be
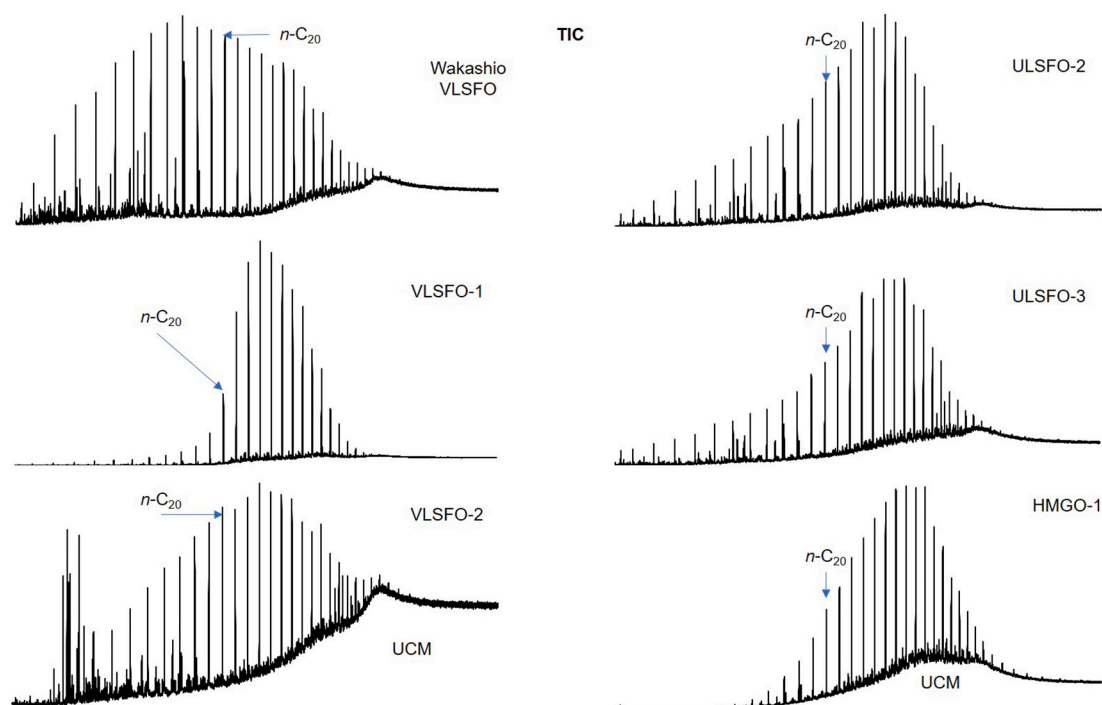
Fig. 1. Full scan GC–MS Total Ion Chromatograms (TIC) of the saturate fractions of a suite of VLSFOs (< 0.50%S, left panel) and ULSFOs (<0.10% S, right panel). UCM = unresolved complex mixture of hydrocarbons.

Table 2

Ratios of *n*-alkane and isoprenoid ratios derived from Full Scan GC–MS TIC and GC × GC-FID analyses of IMO-2020 compliant (<0.05% S) and SECA compliant (<0.01% S). Abbreviations defined in Appendix A.

	ESA compliant fuel oils						SECA compliant fuel oils					
	Wakashio		VLSFO-1		VLSFO-2		ULSFO-2		ULSFO-3		HMGO-1	
	GC–MS	GC × GC	GC–MS	GC × GC	GC–MS	GC × GC	GC–MS	GC × GC	GC–MS	GC × GC	GC–MS	GC × GC
n-C17/Pr	1.01	1.03	2.73	2.67	2.87	2.78	1.39	1.52	1.43	1.52	1.87	1.89
n-C18/Ph	3.19	3.26	5.37	4.93	3.11	3.38	3.13	3.21	3.11	3.20	1.86	1.79
nor-Pr/Pr	0.32	0.33	0.65	0.55	1.21	1.07	0.62	0.48	0.63	0.48	0.83	0.52
Pr/Ph	3.25	3.34	1.45	1.35	1.01	1.11	2.03	2.01	1.93	2.01	0.63	0.61

viewed with caution. Based on this limited range of IMO-2020 compliant oils, there is certainly no obvious similarities between the two classes of oils, i.e. <0.50% S and < 0.10% S, and the differences in chromatograms appear to simply reflect their feedstock oils and, possibly, differences in the refinery processing methods used by different companies.

Hopanoid terpane biomarkers were in low abundances in all of the IMO-2020 compliant oils but profiles were obtained using SIM *m/z* 191 fragmentograms (Fig. 2). These showed clear differences between most of the oils in terms of both presence/absence of specific biomarkers and in the ratios of biomarkers that were common to multiple oils (Table 3). The exception to this was the two ULSFOs which were near identical (Fig. 2, Table 3). Of particular note, was the extremely high ratio of 18α(H)-22,29,30-trisnorneohopane (Ts) to 17α(H)-22,29,30-trisnorhopane (Tm) of 4.4 and corresponding Ts/(Ts + Tm) of 0.82 in VLSFO-1 (Table 3). Although it is possible that co-elution could be affecting the abundance of the *m/z* 191 ion, ratios derived by GC × GC-FID were in very close agreement to the GC–MS SIM values (Table 3) so this is highly unlikely. In an examination of effects due to the processing of feedstock oil into the various refined products by Peters et al. (1992), it was noted that several products, including vacuum gas oil (VGO) and the residium, had elevated Ts/(Ts + Tm) compared with the feedstock, which was attributed to the lower stability of Tm compared to the other terpanoids. The abundance of Tm was particularly low in VLSFO-1 which might be explained by the observations and mechanisms reported by Peters et al.

(1992), but the ratio of Ts to 17α(H),21β(H)-hopane (H) was also high, suggesting that the high abundance of Ts was at least contributing to the extremely high Ts/Tm ratio (Table 3).

Sterane biomarkers were present in even lower abundances but SIM (*m/z* 217, 218) revealed some differences between the oils (Fig. S1). In particular, the near absence in diasteranes in VLSFO-1 but the *m/z* 217 fragmentogram revealed the presence of bicadinanes (Fig. S1) which was confirmed by GC × GC-HRT (see below). These C_{30} pentacyclic triterpanes are angiosperm biomarkers that are mainly derived from terrestrial plants, *Shorea* spp., from the Dipterocarpaceae family that evolved in the Tertiary and slowly spread through Southeast Asia (Vanaarssen et al., 1990). A more detailed comparison of the terpane and sterane biomarkers using GC × GC-HRT is discussed below.

3.2. Characterization of whole oils by high temperature GC-FID

The temperature range of normal GC analysis precludes detection of higher weight components such as *n*-alkanes with >35–40 carbon atoms so HTGC-FID of the whole fuel oils was used to extend the analysis range. Without additional wax refinement, our data likely provides an underestimate of *n*-alkane distributions. All of the oils possessed *n*-alkanes >C_{40} with ULSFO-2 extending up *n*-C_{65} (Fig. S2a). However, none of the IMO-2020 compliant oils had substantial quantities of *n*-alkanes exceeded that of a heavy fuel oil analysed for comparison and VLSFO-1
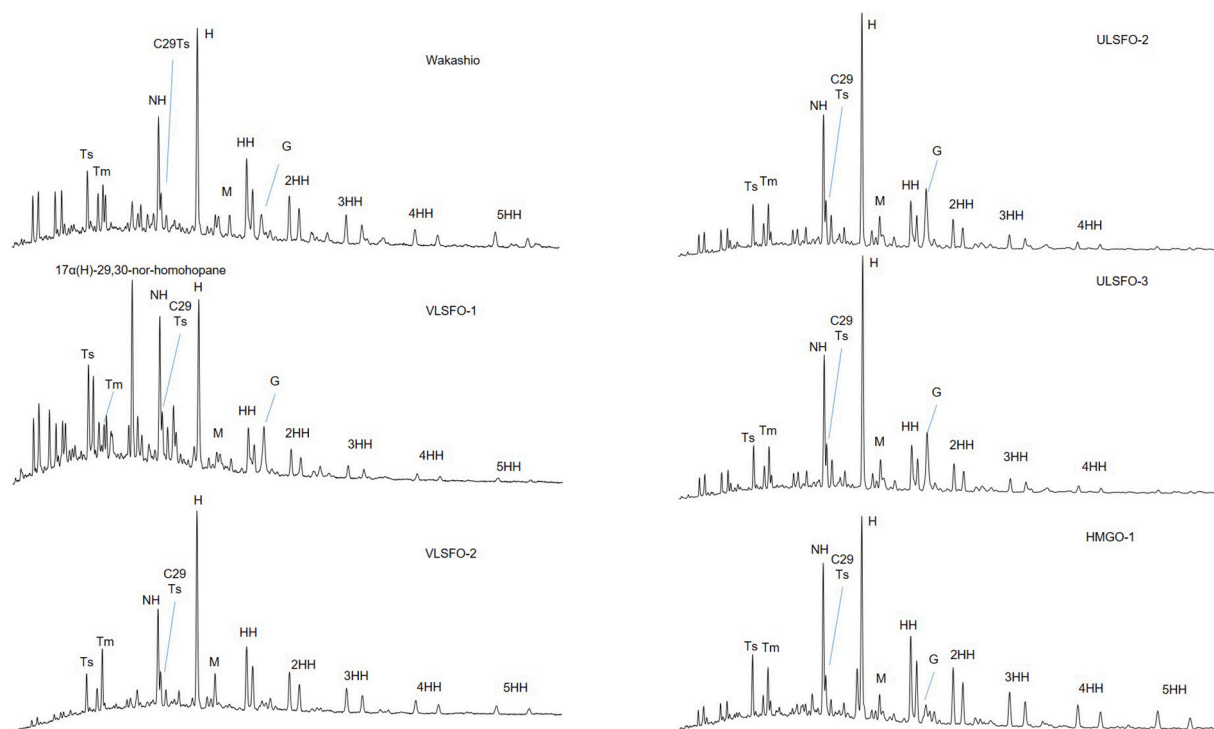
Fig. 2. Hopanoid biomarkers present in a suite of VLSFOs (< 0.50% S, left panel) and ULSFOs (<0.10% S, right panel) derived from GC–MS selected ion monitoring (*m/z* 191). Abbreviations defined in Appendix A.

Table 3
Comparison of key terpane biomarker ratios derived from GC–MS SIM (m/z 191) of saturates fraction and GC × GC-FID analyses of whole fuel oils.

Ratio	IMO-2020 compliant fuel oils						SECA compliant fuel oils					
	Wakashio		VLSFO-1		VLSFO-2		ULSFO-2		ULSFO-3		HMGO-1	
	SIM	GC × GC	SIM	GC × GC	SIM	GC × GC	SIM	GC × GC	SIM	GC × GC	SIM	GC × GC
Ts/Tm	1.19	1.56	4.41	4.51	0.66	0.71	1.10	1.26	1.10	1.30	1.39	1.53
Ts/(Ts + Tm)	0.54	0.61	0.82	0.82	0.40	0.41	0.52	0.56	0.52	0.56	0.58	0.61
Ts/H	0.21	0.29	0.46	0.68	0.15	0.21	0.14	0.21	0.15	0.22	0.22	0.32
Tm/H	0.17	0.18	0.10	0.15	0.23	0.29	0.13	0.16	0.13	0.17	0.16	0.21
C29-Ts/H	0.17	0.22	0.27	0.35	0.07	0.23	0.17	0.25	0.17	0.25	0.18	0.24
NH/H	0.44	0.57	0.79	0.91	0.36	0.57	0.54	0.61	0.54	0.62	0.65	0.78
NM/H	n/a	0.05	n/a	0.07	0.06	0.12	n/a	0.10	n/a	0.09	n/a	0.10
M/H	0.11	0.04	0.07	0.04	0.16	0.11	0.10	0.26	0.10	0.26	0.10	0.09
O/H	n/a	n/a	0.13	0.10	n/a	0.05	n/a	0.04	n/a	0.04	0.29	0.37
HH(S)/H	0.49	0.49	0.27	0.34	0.36	0.46	0.27	0.27	0.27	0.24	0.48	0.62
HH(R)/H	0.28	0.37	0.14	0.30	0.28	0.35	0.16	0.21	0.15	0.18	0.34	0.49
G/H	0.16	0.02	0.44	0.11	0.00	0.02	0.43	0.15	0.43	0.12	0.14	0.05
2HH(S)/H	0.24	0.37	0.16	0.22	0.22	0.32	0.14	0.20	0.14	0.18	0.29	0.45
2HH(R)/H	0.18	0.25	0.11	0.18	0.16	0.23	0.11	0.14	0.11	0.13	0.23	0.33
3HH(S)/H	0.16	0.25	0.11	0.13	0.15	0.23	0.08	0.11	0.07	0.09	0.21	0.33
3HH(R)/H	0.07	0.15	0.06	0.08	0.10	0.16	0.04	0.07	0.04	0.06	0.15	0.22
4HH(S)/H	0.11	0.19	0.05	0.07	0.08	0.15	0.05	0.06	0.04	0.05	0.16	0.25
4HH(R)/H	0.07	0.10	0.04	0.04	0.05	0.09	0.03	0.04	0.02	0.03	0.12	0.16
5HH(S)/H	0.10	0.19	n/a	0.05	n/a	0.12	n/a	0.04	n/a	0.03	0.14	0.22
5HH(R)/H	0.05	0.11	n/a	0.03	n/a	0.08	n/a	0.02	n/a	0.01	0.07	0.15

only possessed detectable *n*-alkanes up to *n*-C_{42} (Fig. S2b), using the method employed herein. Sørheim et al. (2020, 2021) reported the wax content for the IMO-2020 compliant oils (reproduced in Table 1). This showed ULSFO-2 to have the highest wax content of 20.7% which was considerably higher than the other IMO-2020 compliant oils and typical HFOs (Table 1). The high weight components result in increased viscosities and pour point temperatures such that ULSFO-2 has a pour point of 24 °C (Sørheim et al., 2020) which is above the average global sea surface temperature and greater than most regions outside of the tropics (Scripps, 2014). Hence, spillages of IMO-2020 compliant oils in many areas of the world's oceans and seas will likely result in the formation of

very sticky slicks and emulsions that may impact wildlife and make clean-up operations difficult.

3.3. Overview of whole oils by GC × GC-FID

Two-dimensional chromatograms can be viewed as 'mountain plots' in which the peaks of individual compounds are seen projecting upwards with increasing abundance and separated by boiling point/vapor pressure in the primary dimension (separation by long non-polar column) and by polarity in the secondary dimension (separation by short mid-polar column). A comparison of whole oils by GC × GC-FID (Fig. 3)

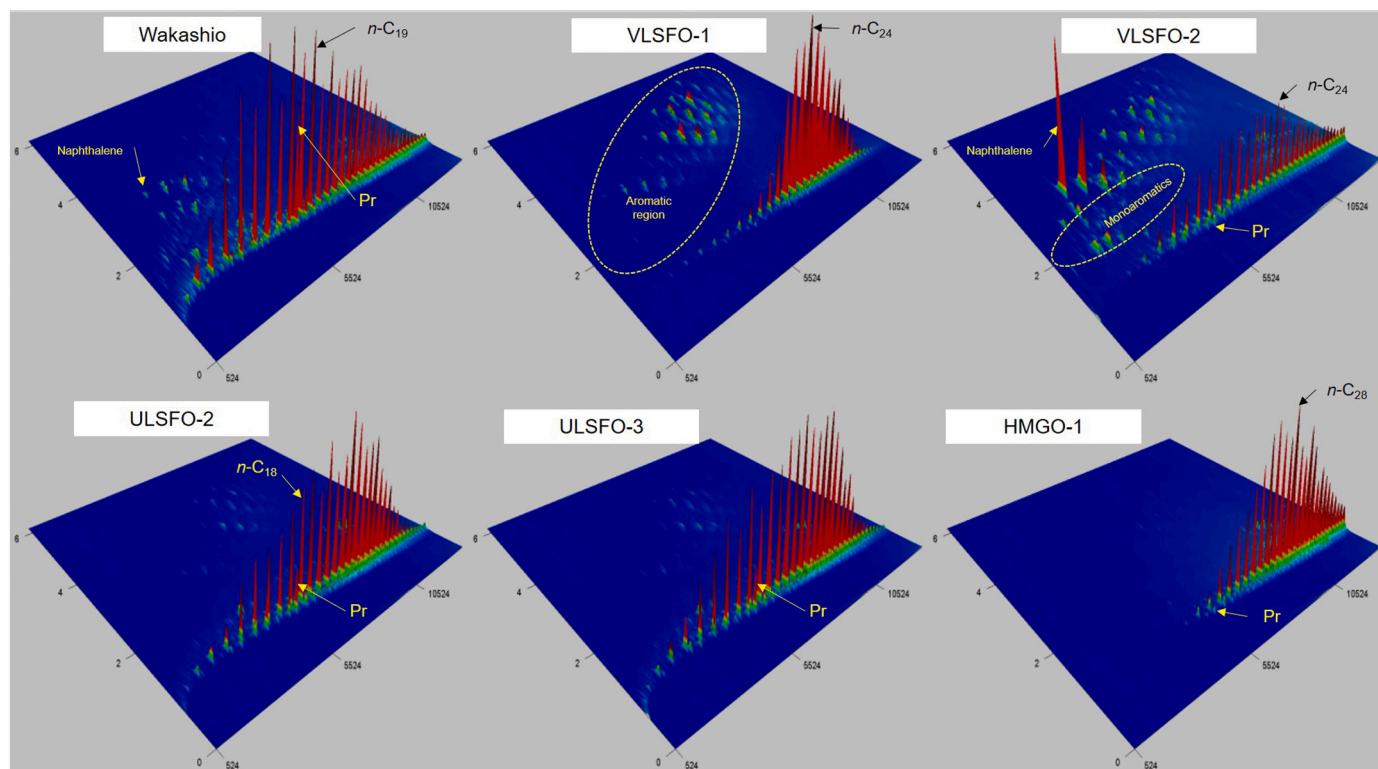**Fig. 3.** GC × GC-FID 'mountain plot' chromatograms of whole oils showing elution positions of selected *n*-alkanes (*n*-C$_x$), pristane (Pr) and aromatic region.

showed that as well as clear differences in alkane profiles as evident using GC–MS (Fig. 1), there was also considerable variation in the aromatic region of the oils. Scarlett et al. (2021) reported that the PAH content of the *Wakashio* VLSFO was relatively low compared to many HFOs (Uhler et al., 2016). A very detailed comparison of individual PAH concentrations in VLSFO-1, VLSFO-2 and ULSFO-2 was reported by Sørheim et al. (2020). This revealed considerable variation in PAH concentrations, with VLSFOs in the ranges reported for 71 HFOs by Uhler et al. (2016) but the ULSFO had close to or below the minimum reported concentrations.

When viewed as mountain plots, aromatic compounds were particularly prominent in VLSFO-2 where the naphthalene peak exceeded that of the *n*-alkanes (Fig. 3). This is a highly unusual feature in residual fuel oils and may result from catalytic processing. One method of reducing the sulfur and nitrogen content in fuel oils is hydrotreating the VGO distillation cut in conjunction with a catalyst, referred to as hydrofining (Peters et al., 1992). This process results in the release of bound compounds including aromatics, so it is possible that this unusual feature is due to the catalytic process used to reduce the S and N content in the IMO-2020 compliant fuels. Low molecular weight monoaromatics e.g. alkylbenzenes, indanes and tetralins were also visible in the chromatogram (Fig. 3). These toxic mono- and diaromatic compounds would typically be rapidly lost due to evaporative processes in warm climates but could persist in colder regions, such as Arctic and Antarctic waters, where the unusually high parent naphthalene could potentially be diagnostic. Triaromatic compounds, including phenanthrenes, were prominent peaks in the chromatogram of VLSFO-1 (Fig. 3). Potential diagnostic features of alkylphenanthrenes/anthracenes are discussed below in the GC × GC-HRT section. So, in terms of VLSFOs, the *Wakashio* oil spilled in Mauritius in 2020 is perhaps not typical and other oils of this class analysed herein, could potentially pose a greater threat to organisms via toxic aromatic compounds if spilled. In contrast, the chromatograms of all the <0.10% S oils showed negligible peaks in the aromatic elution region (Fig. 3) which is in agreement by data reported by Sørheim et al. (2020).

3.4. Biomarkers in whole oils analysed by GC × GC-FID

The chromatographic resolving power of GC × GC-FID make it ideal for quantification of biomarker ratios, especially when used in conjunction with GC × GC-HRT which permits additional mass spectral identification of closely eluting peaks (Nelson et al., 2019). In general, the biomarker ratios derived by GC × GC-FID were similar to those derived by GC–MS (Table 3) but provided greater confidence due to the improved peak resolution reducing possible co-elutions. Chromatograms of the biomarker region of the oils, produced by GC × GC-FID, are shown in Fig. S3. A 'Radar chart' (aka Spider plot) of the principal GC × GC-FID biomarker ratios aids visualization of the similarities and differences between the oils (Fig. 4). Biomarker data from the spilled oil collected in Mauritius (Scarlett et al., 2021) was included in the plot which revealed, as expected, that this was aligned with that of the *Wakashio* VLSFO (Fig. 4). Similarly, the profiles of the two ULSFOs also overlapped. The Radar chart also showed that VLSFO-1 and HMGO-1 were markedly different from the other oils and from each other (Fig. 4). This was further explored using GC × GC-HRT.

3.5. Characterization of biomarkers in whole oils by GC × GC-HRT

A detailed examination of the biomarker region of the IMO-2020 compliant oils using the enhanced chromatographic resolving power and high mass spectral resolution of GC × GC-HRT revealed distinct differences between the oils, which could aid identification following an oil spillage. For example, the VLSFO-1 contained a series of peaks with mass spectra consistent with diahopanes eluting below the plane of the normal hopanes in the second (polar) dimension (Fig. S4a). Also in this plane was an unusually high peak of tentatively assigned 17α(H)-29,30-nor-homohopane and a smaller peak assigned as 17α(H)-30-nor-29-homohopane (Fig. S4). The former was also visible by GC–MS SIM *m/z* 191 fragmentogram (Fig. 2) but the GC × GC-HRT mass spectrum (Fig. 3b) was much cleaner and therefore fragment ions resulting from co-elution could be eliminated. VLSFO-1 was also the only analysed
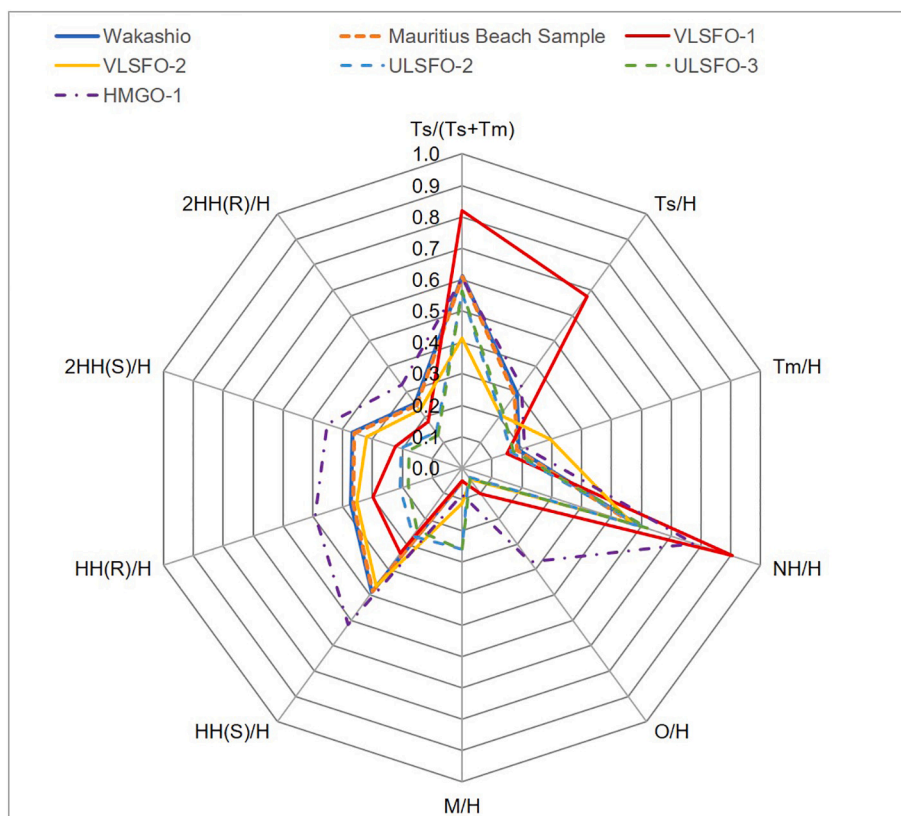
Fig. 4. Radar chart showing the similarities and differences in the GC × GC-FID biomarker profiles of a suite of VLSFOs and ULSFOs, with an oil sample collected from Mauritius following the MV *Wakashio* spillage (biomarker data from Scarlett et al., 2021) used as an example of how oils can be rapidly compared.

IMO-2020 compliant oil to contain a suite of pentacyclic non-hopanoid triterpenoids known as bicadinanes (Fig. S5). In 'normal phase' (primary apolar column) GC × GC, the bicadinanes elute well below the pentacyclic hopanoid biomarkers close to the *seco*-hopanes and possess distinctive mass spectra (Fig. S5). The confirmed presence of a significant suite of bicadinanes, including a *homo*-bicadinane (Fig. S5), strongly suggests Southeast Asia as the origin of the feed stock crude oil for this batch of VLSFO-1 (Vanaarssen et al., 1990). This oil also contained a significant oleanane peak (Fig. S4a) which is another specific C_{30} angiosperm biomarker (Baas, 1985) which elutes just before hopane in the apolar dimension and slightly below in the polar dimension (Eiserbeck et al., 2011). However, some of the other oils also contained oleanane (Table 3) so its presence cannot be used as a specific identifier for a particular fuel oil. Peters et al. (1992) reported that the relative abundance of oleanane was increased in both VGO and residium refinery products when compared to their feedstock. It was speculated that the six-membered E-ring of oleanane may enhance its stability relative to the five-membered ring of hopane and moretane (Peters et al., 1992). A comparison by GC × GC-HRT of the biomarker region of ULSFO-2 and ULSFO-3 (Fig. S6) exemplifies the resemblance between these oils, thus confirming the GC–MS and GC × GC-FID analyses (Fig. 2, Table 3) that strongly suggests these two brands of oils are from the same source.

Some of the oils contained 8,14-*seco*hopanes, revealed by extracted ion *m/z* 123.1168. These were more pronounced in VLSFO-1 and, to a lesser degree, in the ULSFOs and *Wakashio* VLSFO but negligible in VLSFO-2 and HMGO-1. VLSFO-1 also contained some small peaks consistent with 2α-methyl-8,14-*seco*hopanes (extracted ion *m/z* 137.1325).

Isomers of steranes are not particularly well separated in the polar dimension by the 2D column configuration used in this study. The separation of the sterane peaks from the column bleed and from other biomarkers, such as hopanes, that possess some common fragment ions,

plus the superior GC × GC-HRT mass spectral resolving power is however useful when examining the diasteranes and steranes present in the fuel oils. The diasteranes were more prominent in the HMGO-1 fuel oil (Fig. S7). C-ring monoaromatic steranes (unique fragment ion *m/z* 253.1951) and triaromatic steroids (unique fragment ion *m/z* 231.117) were also prominent in the latter and, to a lesser extent in and with a quite different profile, *Wakashio* VLSFO (Fig. S8) but negligible or absent in the other fuel oils. Peters et al. (1992) reported that both mono- and tri aromatic steroids were well-preserved during the VGO hydrofining process but not observed in the other refined products, and were in low abundance in the residium. The presence of prominent mono- and tri aromatic steroids could therefore prove diagnostic for distillate SECA compliant fuels.

Although for the IMO-2020 compliant oils analysed herein, sterane and hopane biomarkers were present, albeit with generally low abundance, this might not necessarily be the case for other IMO-2020 compliant oils. In the absence of these higher molecular weight biomarkers, C_{15-16} bicyclic sesquiterpanes can be useful for differentiating oils due to their ubiquitous presence and their resistance to weathering (Alexander et al., 1984; Wang et al., 2006). With the exception of the two ULSFOs, the bicyclic sesquiterpane profiles were sufficiently distinct to be potentially useful for forensic purposes (Fig. S9).

3.6. Characterization of aromatics and heterocyclics in whole oils by GC × GC-HRT

A detailed quantification of PAHs in IMO-2020 compliant oils was reported by Sørheim et al. (2020; 2021) and is not the focus of the current study. A diagnostic feature of fuel oils is the presence of 2-methylanthracene (2-MA) which is only found in trace amounts in crude oils (Uhler et al., 2016). With the exception of HMGO-1, in which the methylphenanthrenes (MP) are in extremely low abundance, all of the

oils contained 2-MA but was more prominent in VLSFO-1 and 2 (Fig. S10). For the oils in which 2-MA was present, the ratios of 2-MA/ΣMP were in the range 0.04–0.08 (by GC–MS, Fig. S10), which is in agreement of that reported by Uhler et al. (2016) for 71 fuel oils. The presence of 2-MA in the fuel oils is consistent with its generation during thermal cracking and can provide a fingerprint of fuel oil as distinct from weathered crude oil (Uhler et al., 2016).

Scarlett et al. (2021) postulated that due to the various methods used to remove the sulfur during the production of IMO-2020 compliant oils, this may result in characteristic profiles of various heterocyclic compounds that could be forensically useful. It appeared that for the *Wakashio* fuel oil, nitrogen-containing compounds may have been removed during the sulfur removal process whereas those containing oxygen were not (Scarlett et al., 2021). Indeed, the refinery process of VGO hydrofining removes, to some extent, both sulfur and nitrogen (Peters et al., 1992), so other catalytic processing of residual fuel oils may also achieve this. It was also observed that the profiles of many isomeric heterocyclics present in the fuel oil were retained in the weathered spilled oil and therefore any differences observed in the suite

of IMO-2020 compliant oils analysed herein are likely to be retained in the event of an oil spill.

In contrast to *Wakashio* VLSFO which has the unusual feature of a prominent dibenzothiophene (DBT) peak with diminishing abundances with increasing alkylation, the other VLSFOs showed more typical greater abundances of the C_{2-4} alkyl homologues and the ULSFOs contained virtually no peaks of the DBT suite (Fig. 5). Phenanthrothiophenes were reported to be in low abundances in the *Wakashio* fuel oil (Scarlett et al., 2021) but VLSFO-1, and to a lesser extent, VLSFO-2 had significant peaks, especially for the alkylated homologues. However, these were very low in ULSFO-2 and not detectable in the HMGO-1 (Fig. S11). Benzonaphthothiophenes and chrysenothiophenes showed the same trend as the phenanthrothiophenes with only VLSFO-1, and to a lesser extent, VLSFO-2 having significant peaks of alkylated homologues. Scarlett et al. (2021) suggested that, based on the *Wakashio* oil spill data, that nitrogen-containing heterocyclics might also be removed during the sulfur removing process. Although this was generally the case for the suite of oils analysed herein, VLSFO-1 was observed to possess significant peaks of carbazoles and benzocarbazoles (Fig. S12) which
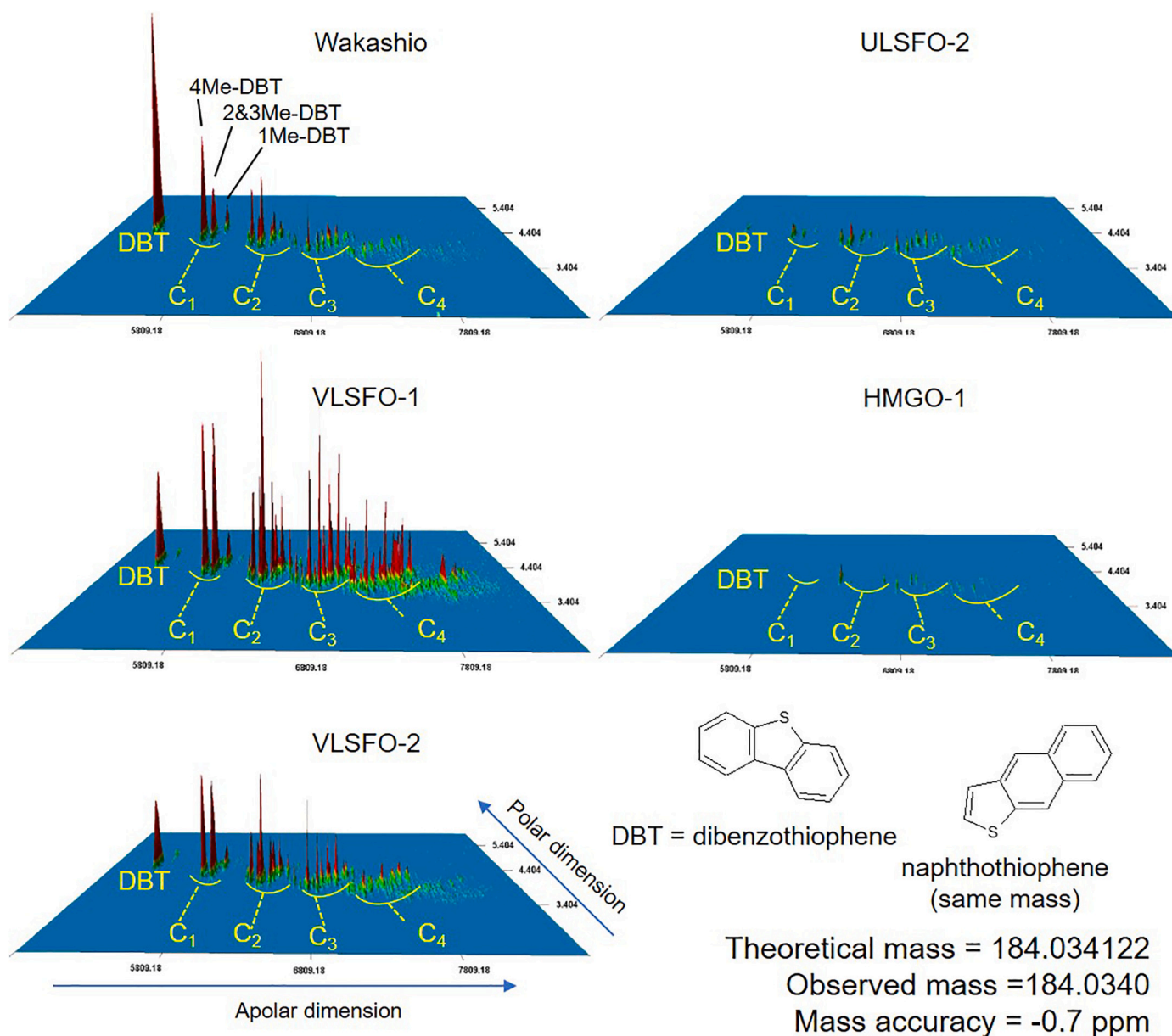

Fig. 5. GC × GC-HRT surface plots comparing dibenzothiophenes (or naphthothiophenes) in a suite of IMO-2020 compliant oils.

might be forensically useful. The hypothesis that oxygen-containing heterocyclics were unaffected by the sulfur removing process (Scarlett et al., 2021), was not supported by the current study. Although dibenzofurans were evident in the *Wakashio* VLSFO, these were less prominent in the other VLSFOs and barely detectable in the ULSFOs (Fig. 6). This could however be forensically useful as a means of differentiating *Wakashio* VLSFO from the other VLSFOs. Heterocyclics of any kind were virtually undetectable in the ULSFOs and HMGO-1, but as the two ULSFOs were near identical in terms of biomarker ratios, generalisations regarding SECA compliant fuels are not justified.

Overall, the evidence from this suite of oils, suggests that suites of heterocyclics can be used to distinguish between VLSFOs and ULSFOs, and between different brands of VLSFOs, and that these profiles could be useful to help identify the origin of the oil. Whether the observed differences result from the sulfur removal processes or, are simply related to the feed stock crude oils remains unclear. A larger dataset would be required to further assess the usefulness of these compounds and studies that include extensive weathering would be useful to confirm that these suites of heterocyclics are not significantly altered following an oil spill.

3.7. Isotopic analysis by GC-irMS

Laboratory studies have suggested that $\delta^{13}C$ ratios are largely unaffected by mild weathering (Asif et al., 2011; Li et al., 2009) but a comparison of the *n*-alkanes between the *Wakashio* fuel oil and that collected from the Mauritius environment following the spill, revealed some small differences for both $\delta^{13}C$ and δ^2H (Scarlett et al., 2021). Such differences are probably too minor to prevent the use of isotopic signatures where large divergences exist between oils, and could therefore be forensically useful. In the present study, we determined the isotopic signatures of *n*-alkanes, pristane and phytane in IMO-2020 compliant oils to explore if forensically useful differences were present. ULSFO-2 possessed *n*-alkanes with the most depleted $\delta^{13}C$ with clear separation between it and the other oils (Fig. 7a). HMGO-1, was also more depleted in $\delta^{13}C$ sufficiently to be distinct from the other oils. However, all of the VLSFOs had fairly similar values which, when subject to weathering, are unlikely to be readily distinguishable. In general, the $\delta^{13}C$ of the isoprenoids pristane and phytane, showed greater similarity between the oils and were therefore less diagnostically useful (Fig. 7a).
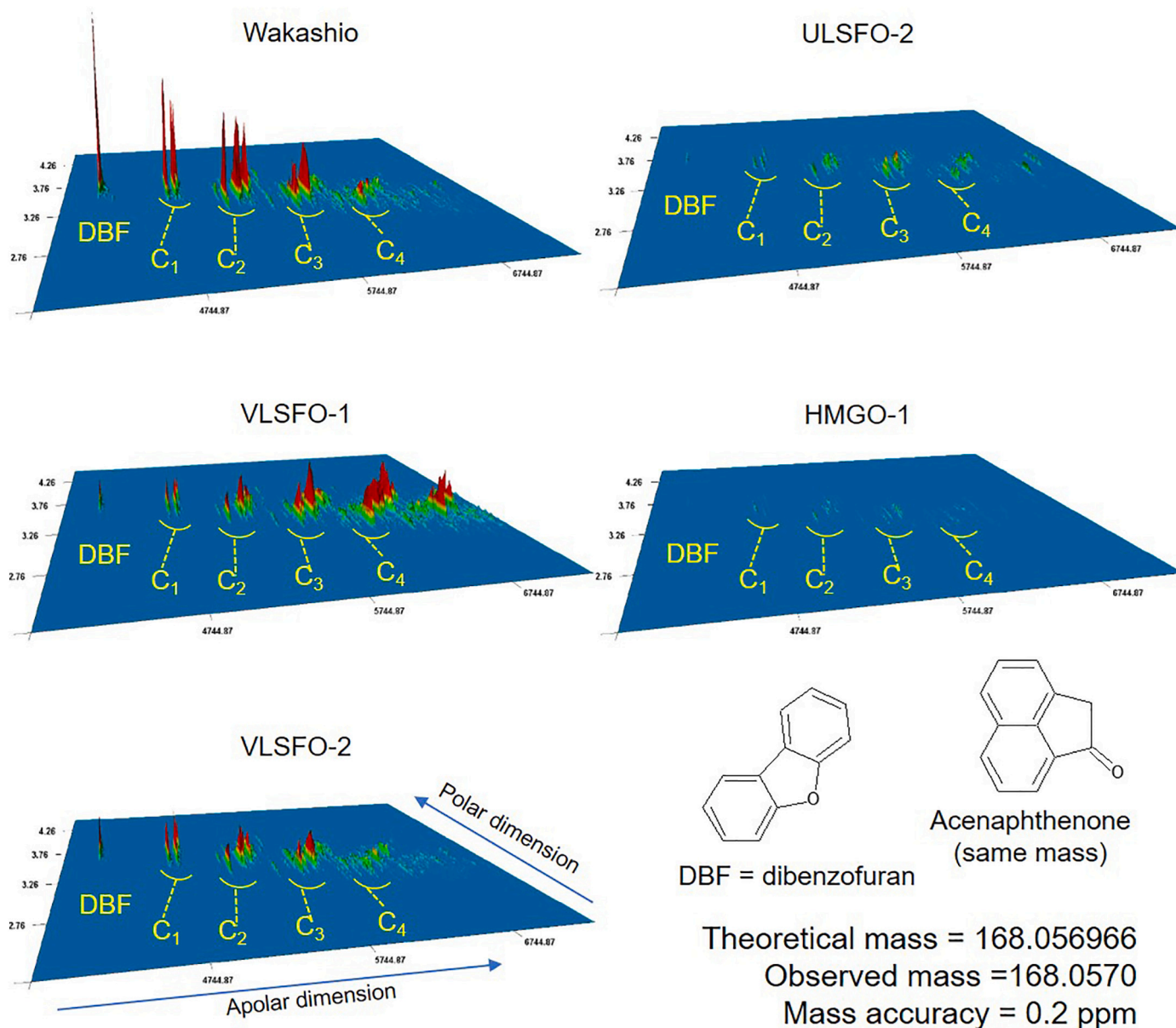

Fig. 6. GC × GC-HRT surface plots comparing dibenzofurans (or acenaphthenones) in a suite of IMO-2020 compliant oils.
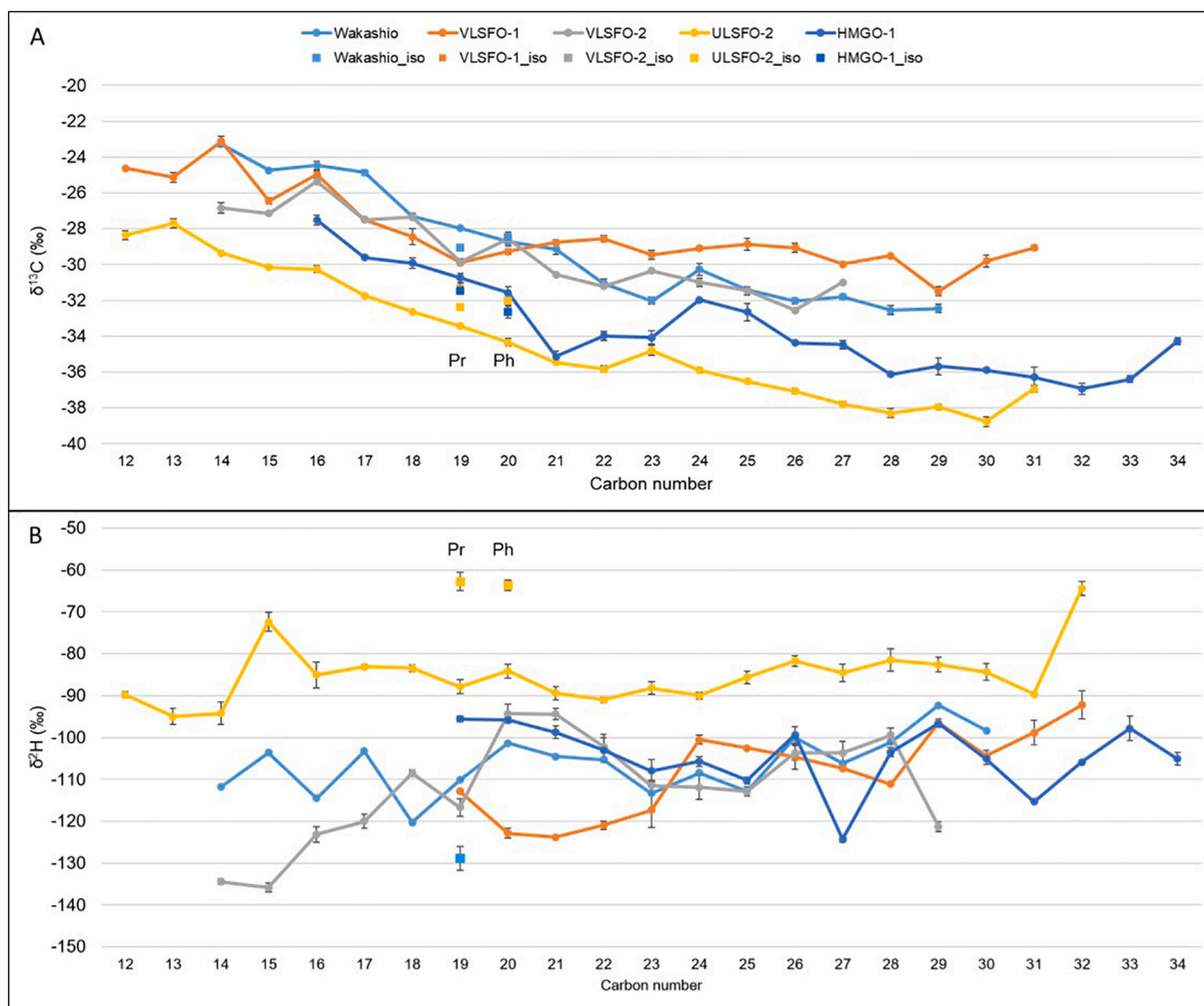
Fig. 7. Stable isotope ratios (A) $\delta^{13}C$ and (B) δ^2H of *n*-alkanes and isoprenoids pristane (Pr) and phytane (Ph) derived from a suite of IMO-2020 compliant oils. Error bars = 1 standard deviation. Note that δ^2H of Pr and Ph could not be measured in all oils.

Comparing δ^2H, the *n*-alkanes of ULSFO-2 was the least depleted i.e. the opposite of that for $\delta^{13}C$ (Fig. 7b). There were sufficient differences between this oil and the others to likely be diagnostic in some spill scenarios. There was however, probably insufficient differences between the δ^2H values of the other oils to be able to differentiate these particular oils. For the isoprenoids, it was only possible to obtain δ^2H values for ULSFO-2 and *Wakashio* VLSFO. In contrast to the $\delta^{13}C$ of the isoprenoids, the differences in δ^2H between the two oils was more extreme than with the *n*-alkanes (Fig. 7b) suggesting that, if measurable, δ^2H values for pristane and phytane could prove forensically useful, especially as these highly branched structures are more resistant to weathering processes.

It was not possible to analyse for $\delta^{13}C$ and δ^2H in ULSFO-3 concurrently with the other oils but it produced δ^2H values similar to ULSFO-2.

3.8. Future work

It is likely that many low-sulfur fuels, current or in development, will share similar compositions due to similarities in their production. Ideally, a study similar to that undertaken by Peters et al. (1992), which tracked the composition of the feedstock through to the different refined products, should be carried out in order to ascertain if compositional changes are common to specific methods used to remove/reduce the sulfur content of the fuel oils. Another approach would be to analyse a much larger suite of oils. This would help build a database of fuels currently in use. In addition, fuel additives could potentially be used as markers but this may require a wider chromatographic window perhaps

best suited to liquid chromatography coupled to high resolution MS.

4. Conclusions

Ratios of commonly used molecular biomarkers derived from both GC–MS and GC × GC-FID analyses, were sufficiently varied between the oils to provide a means of identifying and differentiating these oils should they be spilled in the environment. However, two ULSFOs obtained from different sources proved to be near identical based on their overall characteristics and through our forensic biomarker comparisons. Some biomarkers were common to all oils and were therefore useful for comparisons, whereas some oils possessed unique biomarkers that could help identify specific oils e.g. the diahopanes and the bicadinanes in VLSFO-1, or their origins. Prominent mono- and triaromatic steroids would appear to be indicative of distillate rather than residual based IMO-2020 compliant oils but this would require further testing. Weathering processes tend to increase the relative abundance of biomarkers as lighter components evaporate and more water-soluble components are subject to dissolution, so it is likely that even though the biomarker content of these oils was low, they should still be present in quantities measurable by GC–MS, GC × GC-FID, GC × GC-TOFMS, or GC × GC-HRT following a spill. In addition to the biomarkers, the profiles of several suites of heterocyclics were found to be forensically useful. Although it appeared generally the case that N-containing heterocyclics were in very low abundances consistent with their removal during the sulfur removal process, one oil, VLSFO-1, did possess

significant peaks of carbazoles and benzocarbazoles which perhaps suggests it may have been subject to a different desulfurization process. Although O-containing heterocyclics were prominent in the *Wakashio* VLSFO, this was not the case for the other VLSFOs which again may indicate a different processing method. Our study included three oils with <0.10% S but, as two were deemed to have originated from the same feedstock and processing method, effectively there were only two for comparison with the VLSFOs. These SECA compliant oils were clearly different to all three of the VLSFOs based on their aromatic content and on their S- and O-containing heterocyclics, but additional <0.10% oils would be required in order to ascertain if this was a diagnostic feature. Compound specific stable isotope profiles of *n*-alkanes, pristane and phytane were probably of less use forensically than the biomarkers, although ULSFO-2 was found to be quite distinctive in its relatively low depletion in δ^{13}C combined with its relatively high depletion in δ^2H. Stable isotopes might therefore be of greater use forensically if terpane biomarkers are less abundant.

This study compared fuel oils compliant with the IMO-2020 Global Sulfur Cap from several major fuel oil production companies. Using a range of analytical techniques and various suites of organic compounds, it was possible to differentiate (or match) the oils and this should also be possible following oil spills. A greater range of IMO-2020 compliant oils and different batches of oils from the same manufacturer would need to be studied in order to build a database to aid rapid identification of spilled fuel oils in the environment.

CRediT authorship contribution statement

Alan G Scarlett, Robert K. Nelson, Marthe Monique Gagnon, Christopher M. Reddy, and Kliti Grice conceived the study. Alex I. Holman conducted isotope analyses. Paul A. Sutton conducted high temperature GC analyses. Alan G Scarlett conducted GC–MS analyses. Robert K. Nelson conducted GC × GC–MS analyses. All authors contributed to the writing and editing of the manuscript.

Declaration of competing interest

The authors declare that they have no known competing financial interests or personal relationships that could have appeared to influence the work reported in this paper.

Acknowledgments

Appendix A. Abbreviations used for biomarkers

Compound ID	Compound name	Mass (Da)
Abbreviation		
	Isoprenoids	
Pr	Pristane ($C_{19}H_{40}$)	268
Ph	Phytane ($C_{20}H_{42}$)	282
	Diasteranes and steranes	
DiaC27βα-20S	13β,17α(H)20S-diasterane ($C_{27}H_{48}$)	372
DiaC27βα-20R	13β,17α(H)20R-diasterane ($C_{27}H_{48}$)	372
C27αββ-20R	5α,14β,17β,20R-Sterane ($C_{27}H_{48}$)	372
C27αββ-20S	5α,14β,17β,20S-Sterane ($C_{27}H_{48}$)	372
C29ααα-20R	24-ethyl-5α(H),14α(H),17α(H)-20R-cholestane ($C_{29}H_{52}$)	400
C29αββ-20R	24-ethyl-5α(H),14β(H),17β(H)-20R-cholestane ($C_{29}H_{52}$)	400
C29αββ-20S	24-ethyl-5α(H),14β(H),17β(H)-20S-cholestane ($C_{29}H_{52}$)	400
	Hopanoids	
Ts	18α(H)-22,29,30-trisnorneohopane ($C_{27}H_{46}$)	370
Tm	17α(H)-22,29,30-trisnorhopane ($C_{27}H_{46}$)	370
BNH	17α(H),21β(H)-28,30-bisnorhopane ($C_{28}H_{48}$)	384
NH	17α(H),21β(H)-30-norhopane ($C_{29}H_{50}$)	398
C29-Ts	18α(H),21β(H)-30-norneohopane ($C_{29}H_{50}$)	398
NM	17β(H),21α(H)-30-norhopane ($C_{29}H_{50}$) (normoretane)	398
O	Oleanane ($C_{30}H_{52}$)	412
H	17α(H),21β(H)-hopane ($C_{30}H_{52}$)	412
M	17β(H),21α(H)-hopane ($C_{30}H_{52}$) (moretane)	412
HH (S)	17α(H),21β(H)-22S-homohopane ($C_{31}H_{54}$)	426
HH (R)	17α(H),21β(H)-22R-homohopane ($C_{31}H_{54}$)	426
2HH (S)	17α(H),21β(H)-22S-bishomohopane ($C_{32}H_{56}$)	440
2HH (R)	17α(H),21β(H)-22R-bishomohopane ($C_{32}H_{56}$)	440
3HH (S)	17α(H),21β(H)-22S-trishomohopane ($C_{33}H_{58}$)	454
3HH (R)	17α(H),21β(H)-22R-trishomohopane ($C_{33}H_{58}$)	454
4HH (S)	17α(H),21β(H)-22S-tetrakishomohopane ($C_{34}H_{60}$)	468
4HH (R)	17α(H),21β(H)-22R-tetrakishomohopane ($C_{34}H_{60}$)	468
5HH (S)	17α(H),21β(H)-22S-pentakishomohopane ($C_{35}H_{62}$)	482
5HH (R)	17α(H),21β(H)-22R-pentakishomohopane ($C_{35}H_{62}$)	482

Appendix B. Supplementary data

Supplementary data to this article can be found online at https://doi.org/10.1016/j.marpolbul.2022.113791.

References

Alexander, R., Kagi, R.I., Noble, R., Volkman, J.K., 1984. Identification of some bicyclic alkanes in petroleum. Org. Geochem. 6, 63–72.

Asif, M., Fazeelat, T., Grice, K., 2011. Petroleum geochemistry of the Potwar Basin, Pakistan: 1. Oil-oil correlation using biomarkers, delta C-13 and delta D. Org. Geochem. 42, 1226–1240.

Baas, W.J., 1985. Naturally occurring seco-ring-A-triterpenoids and their possible biological significance. Phytochemistry 24, 1875–1889.

CARB, 2020. California Air Resources Board (CARB) Ocean-Going Vessel (OGV) fuel regulation – July 2009. https://ww3.arb.ca.gov/ports/marinevess/documents/marinenotice20201.pdf.

Chen, H., Nelson, R.K., Swarthout, R.F., Shigenaka, G., de Oliveira, A.H.B., Reddy, C.M., McKenna, A.M., 2018. Detailed compositional characterization of the 2014 Bangladesh furnace oil released into the World's largest mangrove Forest. Energy Fuel 32, 3232–3242.

Eiserbeck, C., Nelson, R.K., Grice, K., Curiale, J., Reddy, C.M., Raiteri, P., 2011. Separation of 18 alpha(H)-, 18 beta(H)-oleanane and Lupane by comprehensive two-dimensional gas chromatography. J. Chromatogr. A 1218, 5549–5553.

Fingas, M., 2016. Oil Spill Science and Technology, 2nd edition. Gulf Professional Publishing, Cambridge, MA, USA.

Frysinger, G.S., Gaines, R.B., Xu, L., Reddy, C.M., 2003. Resolving the unresolved complex mixture in petroleum- contaminated sediments. Environ. Sci. Technol. 37, 1653–1662.

Gaines, R.B., Frysinger, G.S., Hendrick-Smith, M.S., Stuart, J.D., 1999. Oil spill source identification by comprehensive two-dimensional gas chromatography. Environ. Sci. Technol. 33, 2106–2112.

IMO, 2020. International Marine Organization (IMO), Marine Pollution (MARPOL) Annex VI — as amended. IMO Protocol of 1997, as amended by resolution MEPC.176(58) in 2008, to amend the International Convention for the Prevention of Pollution from Ships, 1973, as modified by the Protocol of 1978 related thereto. https://www.imo.org/en/About/Conventions/Pages/International-Convention-for-the-Prevention-of-Pollution-from-Ships-(MARPOL).aspx.

Jernelov, A., 2010. How to defend against future oil spills. Nature 466, 182–183.

Lemkau, K.L., Peacock, E.E., Nelson, R.K., Ventura, G.T., Kovecses, J.L., Reddy, C.M., 2010. The M/V cosco Busan spill: source identification and short-term fate. Mar. Pollut. Bull. 60, 2123–2129.

Li, Y., Xiong, Y.Q., Yang, W.Y., Xie, Y.L., Li, S.Y., Sun, Y.G., 2009. Compound-specific stable carbon isotopic composition of petroleum hydrocarbons as a tool for tracing the source of oil spills. Mar. Pollut. Bull. 58, 114–117.

Nelson, R.K., Kile, B.M., Plata, D.L., Sylva, S.P., Xu, L., Reddy, C.M., Gaines, R.B., Frysinger, G.S., Reichenbach, S.E., 2006. Tracking the weathering of an oil spill with comprehensive two-dimensional gas chromatography. Environ. Forensic 7, 33–44.

Nelson, R.K., Aeppli, C., Samuel, J., Chen, H., de Oliveira, A.H.B., Eiserbeck, C., Frysinger, G.S., Gaines, R.B., Grice, K., Gros, J., Hall, G.J., Koolen, H.H.F., Lemkau, K.L., McKenna, A.M., Reddy, C.M., Rodgers, R.P., Swarthout, R.F., Valentine, D.L., White, H.K., 2016. Applications of comprehensive two-dimensional gas chromatography (GC × GC) in studying the source, transport, and fate of petroleum hydrocarbons in the environment. In: Stout, S.A., Wang, Z. (Eds.), Standard Handbook Oil Spill Environmental Forensics Fingerprinting and Source Identification, 2nd ed. Academic Press, Cambridge, MA,USA.

Nelson, R.K., Gosselin, K.M., Hollander, D.J., Murawski, S.A., Gracia, A., Reddy, C.M., Radovic, J.R., 2019. Exploring the complexity of two iconic crude oil spills in the Gulf of Mexico (Ixtoc I and Deepwater Horizon) using comprehensive two-dimensional gas chromatography (GC x GC). Energy Fuel 33, 3925–3933.

Peters, K.E., Scheuerman, G.L., Lee, C.Y., Moldowan, J.M., Reynolds, R.N., Pena, M.M., 1992. Effects of refinery processes on biological markers. Energy Fuel 6, 560–577.

Peters, K.E., Walters, C.C., Moldowan, J.M., 2005. The Biomarker Guide: Volume 1, Biomarkers and Isotopes in the Environment and Human Histor. Cambridge University Press, Cambridge, England.

Peters, K.E., Walters, C.C., Moldowan, J.M., 2007. Biomarker Guide. The. Cambridge University Press, Cambridge, UNITED KINGDOM.

Radovic, J.R., Aeppli, C., Nelson, R.K., Jimenez, N., Reddy, C.M., Bayona, J.M., Albaiges, J., 2014. Assessment of photochemical processes in marine oil spill fingerprinting. Mar. Pollut. Bull. 79, 268–277.

Rowland, S.J., Scarlett, A., West, C., Jones, D., Frank, R., 2011. Diamonds in the rough: identification of individual naphthenic acids in oil sands process water. Environ. Sci. Technol. 45, 3154–3159.

Scarlett, A.G., Nelson, R.K., Gagnon, M.M., Holman, A.I., Reddy, C.M., Sutton, P.A., Grice, K., 2021. MV wakashio grounding incident in Mauritius 2020: the world's first major spillage of very low sulfur fuel oil. Mar. Pollut. Bull. 171, 112917.

Scripps, 2014. Voyager: how long until ocean temperature goes up a few more degrees? Scripps Institution of Oceanography. https://scripps.ucsd.edu/news/voyager-how-long-until-ocean-temperature-goes-few-more-degrees.

Sørheim, K.R., Daling, P.S., Cooper, D., Buist, I., Faksness, L., Altin, D., Pettersen, T., Bakken, O.M., 2020. Characterization of Low Sulfur Fuel Oils (LSFO) – a new generation of marine fuel oils - OC2020 A-050. https://hdl.handle.net/11250/2655946. Trondheim, NORWAY, p. 112.

Sørheim, K.R., Pettersen, T., M, J., 2021. In: Physico-chemical Characterization and Weathering Properties of IM-5 Wakashio. SINTEF, Trondheim, Norway, p. 56. https://hdl.handle.net/11250/2739104.

Uhler, A.D., Stout, S.A., Douglas, G.S., Healey, E.M., Emsbo-Mattingly, S.D., 2016. 13 - Chemical character of marine heavy fuel oils and lubricants. In: Stout, S.A., Wang, Z. (Eds.), Standard Handbook Oil Spill Environmental Forensics, Second edition. Academic Press, Boston, pp. 641–683.

Vanaarssen, B.G.K., Cox, H.C., Hoogendoorn, P., Deleeuw, J.W., 1990. A cadinene biopolymer in fossil and extant dammar resins as a source for cadinanes and bicadinanes in crude oils from south east-asia. Geochim. Cosmochim. Acta 54, 3021–3031.

Wang, Z., Stout, S.A., Fingas, M., 2006. Forensic fingerprinting of biomarkers for oil spill characterization and source identification. Environ. Forensic 7, 105–146.

Wang, Z., Yang, C., Yang, Z., Brown, C.E., Hollebone, B.P., Stout, S.A., 2016. 4 - Petroleum biomarker fingerprinting for oil spill characterization and source identification. In: Stout, S.A., Wang, Z. (Eds.), Standard Handbook Oil Spill Environmental Forensics, Second edition. Academic Press, Boston, pp. 131–254.